

# Crystallization and morphology of a bacterial thermoplastic: poly-3-hydroxybutyrate

P. J. BARHAM, A. KELLER, E. L. OTUN

*H. H. Wills Physics Laboratory, University of Bristol, Tyndall Avenue, Bristol, UK*

P. A. HOLMES

*ICI Agricultural Division, PO Box 1, Billingham, Cleveland, UK*

This paper presents a number of interesting results on the physical properties of poly-3-hydroxybutyrate (PHB). Data are presented on crystallization kinetics, morphology of melt- and solution-crystallized PHB, the variation of lamellar thickness with crystallization temperature, and the assessment of some thermodynamic quantities. These properties include surface free energies, heat of fusion and melting, and glass transition temperatures. It is shown that the special properties of PHB such as the large spherulite size, which is probably due to its exceptional purity, make it an ideal material for model studies of polymer crystallization and morphology. For example, we show that the variation of growth rate with crystallization temperature is consistent with the very latest theories; and that the single crystal morphology has important implications for the understanding of crystal growth in other polymer systems.

## 1. Introduction

Poly *D*(-)-3-hydroxybutyrate (PHB) is an optically active aliphatic polyester produced by many types of micro-organisms. It was first isolated about 50 years ago by Lemoigne [1] and subsequent work has shown that the polymer serves as an energy and carbon storage product in much the same way as glycogen in mammalian tissue [2].

PHB is relatively abundant in the environment and may be found in soil bacteria [3], estuarine micro-flora [4], blue-green algae [5] and microbially treated sewage [6]. The percentage of PHB in these cells is normally low, between 1 and 30%, but under controlled fermentation conditions of carbon excess and nitrogen limitation overproduction of polymer can be encouraged and yields increased to about 70% of dry cell weight [7]. In all cases the polymer occurs as discrete granules within the living organisms and may be extracted from them using a variety of organic solvents such as chloroform [8], ethylene dichloride [9], methylene chloride [10], pyridine [11] and propylene carbonate [12].

There are surprisingly few published works concerning the physical properties of such a common and readily available polymer. We give below a very brief survey of some of the principle findings of previous workers as they relate to the solid state. PHB is a thermoplastic material with a melting point of *c.* 180°C [13] and on cooling slowly from the melt, will crystallize to form large spherulites. Alternatively it may be quenched to a glassy state with  $T_g$  *c.* 5°C or precipitated from dilute solution to produce thin lamellar crystals. The variation of the lamellar thickness with polymer molecular weight has been studied in detail by Marchessault *et al.* [14]. However, the majority of published work on the solid state properties of PHB have been concerned with careful and accurate determination of the crystal structure [15-17], rather than studies of morphological features.

Recently ICI Agricultural Division have developed a pilot scale facility for the production of PHB [18]. Polymers with molecular weights in the range 10 000 to 1 000 000 and with  $M_w/M_n$

approximately 2 are now available in multi-kilogram batches. The product is also exceptionally pure as a result of the biosynthetic process and solvent-based extraction and purification procedures. Unlike conventional thermoplastics, there are no catalyst residues in the polymer. The major impurities are inorganic nitrogen, phosphorus and sulphur-containing compounds.

Thus the level of heterogeneous nuclei present in pure PHB from ICI is very low and very large spherulites with diameters of several centimetres may readily be grown by cooling from the melt. Such large spherulites are unique in our experience of polymers and offer the opportunity to carry out some novel studies. We have taken advantage of this fact to study the nucleation and crystallization kinetics of PHB and the effect of nucleating agents on these processes, this latter study being reported in detail elsewhere [19]. The results of the preliminary studies are reported here. The main purpose of this paper is to serve as an introduction to PHB as a model polymer for studies of morphology and crystallization, and to give values of some of the fundamental constants (e.g. heat of fusion, surface free energies, etc.) for PHB which are needed for such studies.

## 2. Experimental details and results

### 2.1. Fermentation and polymer recovery

The polymer used in this study was synthesized by the continuous fermentation of a glucose-utilizing mutant of *Alcaligenes eutrophus* at a dilution rate of  $0.1 \text{ h}^{-1}$  [20]. The biomass produced was first mechanically dewatered by centrifugation and then spray-dried to give a dry powder containing approximately 55% PHB by weight. This was then washed with hot methanol for 10 min to remove phospholipids, which would otherwise coextract with the polymer and contaminate the product. After redrying, the bacterial cells were refluxed with chloroform for 10 min and a clear polymer solution recovered by centrifugation to remove the majority of the cell debris, followed by a polishing filtration through a  $5 \mu\text{m}$  pore size cartridge filter. Pure polymer was finally obtained by precipitating the solution into methanol, filtering and drying *in vacuo* at  $60^\circ \text{C}$  for at least 24 hours.

### 2.2. Molecular weight determination

The molecular weights quoted in this paper were

obtained by gel permeation chromatography at  $30^\circ \text{C}$  in chloroform using a set of five ( $10^6$ ,  $10^6$ ,  $10^5$ ,  $10^4$ ,  $10^3$ , Å) microstiyragel columns (Polymer laboratories, Church Stretton) with a Wilks Miran infra-red detector. Data accumulation and processing was performed on-line by a Commodore PET micro-computer and the system was calibrated using polystyrene standards. The results were corrected to true molecular weights using the Mark Houwink relationship:

$$\{\eta\} = KM^\alpha \quad (1)$$

For polystyrene in chloroform  $K = 0.49 \times 10^{-4}$  and  $\alpha = 0.794$  [21], while the equivalents for PHB in chloroform are  $K = 1.18 \times 10^{-4}$  and  $\alpha = 0.78$  [22]. Thus true PHB molecular weights are obtained from the polystyrene equivalent by applying a logarithmic shift factor of  $-0.213$ .

### 2.3. The spherulitic morphology of PHB

When PHB is crystallized from the melt it forms banded spherulites, the band spacing depending on the crystallization temperature; in general it is smaller at lower crystallization temperatures.

In Fig. 1 we show a series of optical micrographs of PHB spherulites crystallized at a variety of temperatures after melting at  $200^\circ \text{C}$  for 1 min. The polymer used in this series had  $M_n = 133\,000$ ; and  $M_w = 358\,000$ . The decrease in spherulite diameter due to an increase in nucleation rate as the crystallization temperature is reduced can clearly be seen in this series, as can the large changes in band spacing. The variation in band spacing with crystallization temperature is plotted in Fig. 2 and the variation of diameter in Fig. 3 (further details of this are given in [19]).

The spherulite morphology is also affected by the molecular weight of the polymer. This is illustrated by the micrographs of Fig. 4. We present in Fig. 4 a series of optical micrographs showing the effect of molecular weight on the appearance of the spherulites grown at a crystallization temperature of  $100^\circ \text{C}$ . In general we may say that a lower molecular weight polymer gives a similar morphology to that obtained at higher crystallization temperatures, when using a higher molecular weight material.

We can take advantage of the particularly large spherulite size to obtain selected area X-ray diffraction patterns from parts of the spherulites, and hence we are able to deduce the orientation of the crystal axes within the spherulite. A typical

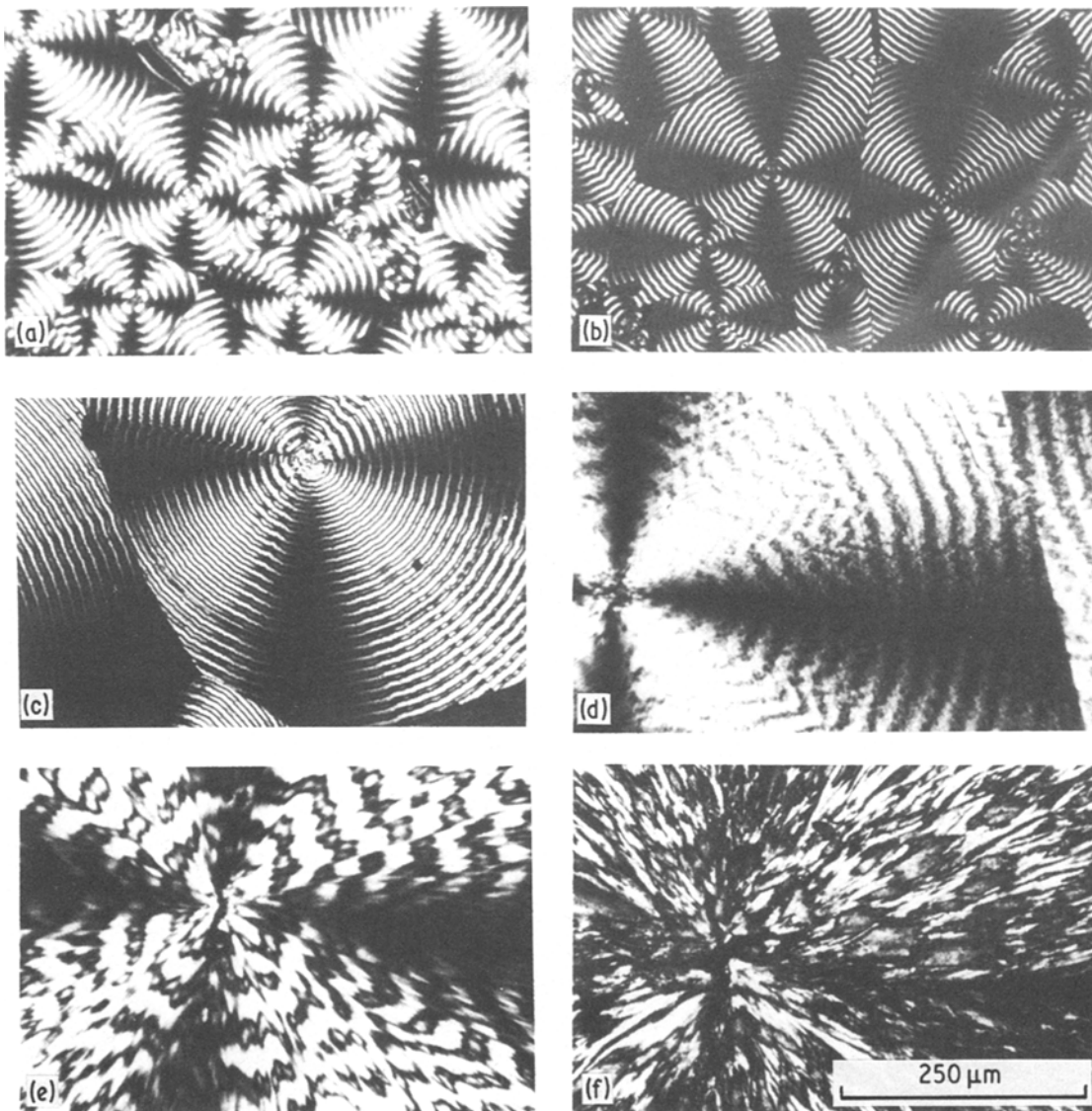


Figure 1 A series of optical micrographs showing how the spherulitic morphology of PHB varies with crystallization temperature (the polymer had  $M_w = 35800$  and  $M_n = 133000$ ). (a)  $T_c = 30^\circ\text{C}$ ; (b)  $T_c = 50^\circ\text{C}$ ; (c)  $T_c = 65^\circ\text{C}$ ; (d)  $T_c = 90^\circ\text{C}$ ; (e)  $T_c = 100^\circ\text{C}$ ; (f)  $T_c = 130^\circ\text{C}$ . Scale as on (f).

diffraction pattern taken near the boundary of a large spherulite is shown in Fig. 5. One feature of Fig. 5 is the wide variation in the line widths; the  $hk0$  reflections being sharp while the others are quite broad due, presumably, to the small lamellar thickness. From such patterns we have concluded that the crystallographic  $a$ -axis is radial in the spherulites and that the other two axes rotate about  $a$ . For clarity we have reproduced a diagram showing the orientation of the PHB molecules in the crystal unit cell together with a sketch of the arrangement of crystallographic

axes within a spherulite in Fig. 6. We have further been able to deduce the actual orientation of the  $b$ - and  $c$ -axes within each band, as indicated on Fig. 6, from measurements of the sign of birefringence.

We have also measured the radial growth rates and lamellar thicknesses of PHB spherulites as a function of crystallization temperature. Growth rates were measured directly using a Mettler hot stage in the optical microscope. Lamellar thicknesses were measured from low angle X-ray diffraction patterns obtained from thin ( $\sim 100\mu\text{m}$ )

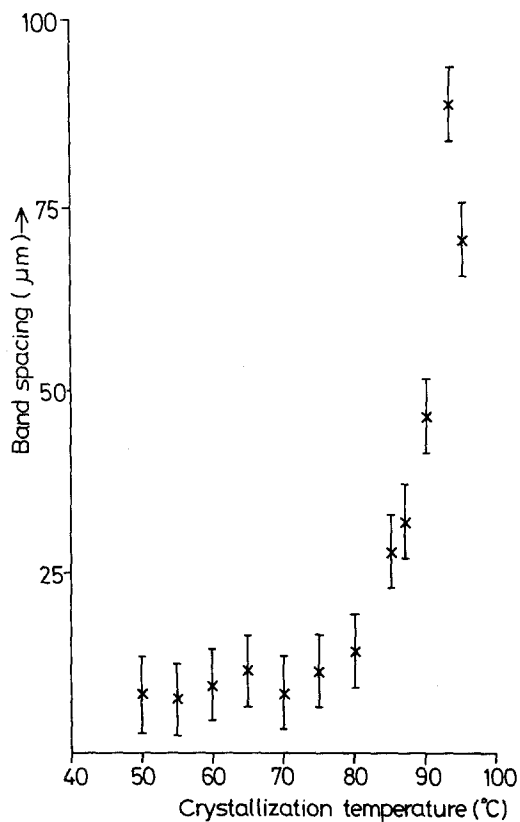


Figure 2 A graph showing the variation in band spacing on PHB spherulites as a function of crystallization temperature.

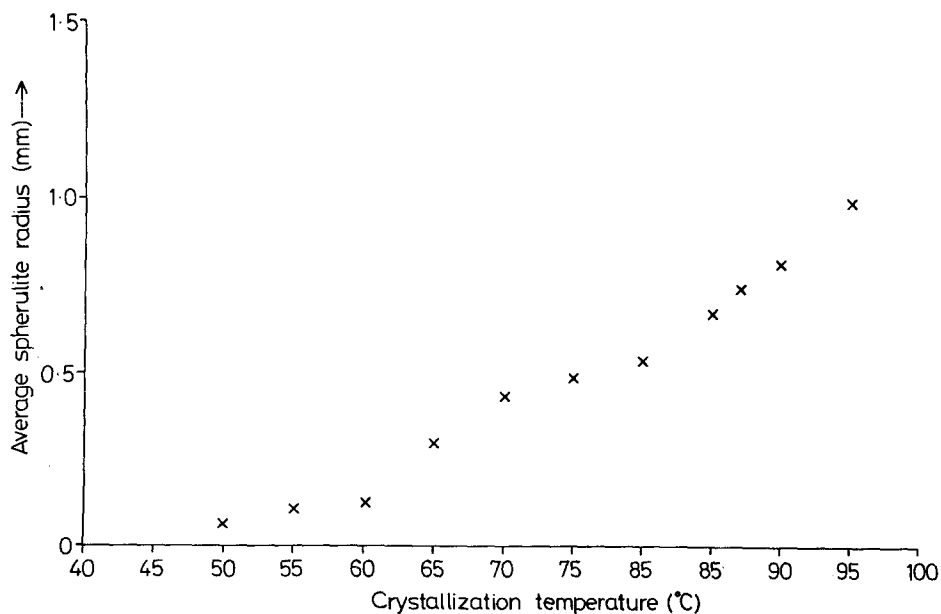
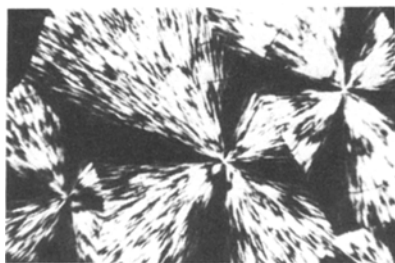


Figure 3 A graph showing the variation of the average radius of PHB spherulites as a function of their crystallization temperature.

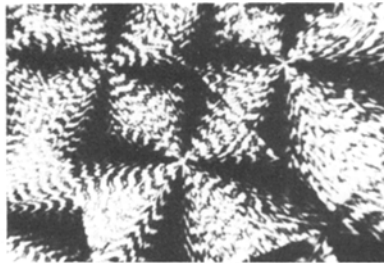
samples, which had been fully crystallized by quenching from the melt into an oil or water bath at the crystallization temperature, and left there (for several days) until crystallization was complete. We show in Fig. 7 a graph of the measured growth rates as a function of crystallization temperature, and in Fig. 8 we present the results of the studies of lamellar thickness.

#### 2.4. Solution-grown crystals

It is possible to grow single crystals of PHB from dilute solutions. Electron micrographs of such crystals grown from mixed solvent systems have been published by Marchessault *et al.* [14]. We are currently undertaking a programme of research to study in detail the morphology of PHB single crystals grown from a variety of solvents over a wide temperature range. The principal difficulty in this study is the high sensitivity of PHB to beam damage in the electron microscope. We show in Fig. 9 a series of electron micrographs showing typical crystals of PHB grown at various temperatures between 30° C and 90° C (the crystals have been shadowed with Pt/Pd to improve contrast). It is particularly noticeable that the crystals always appear to have an elongated arrow-like shape, although the edges are often quite rough (particularly at the lower growth temperatures). In some



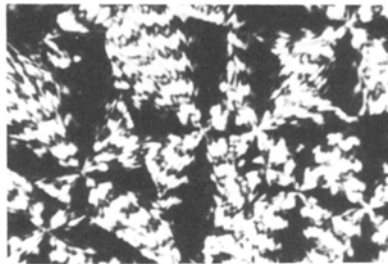
$M_w = 35,000$   
 $M_n = 20,000$



$M_w = 180,000$   
 $M_n = 73,000$



$M_w = 358,000$   
 $M_n = 133,000$



$M_w = 468,000$   
 $M_n = 250,000$

1mm

Figure 4 A series of optical micrographs showing the variation in the spherulitic morphology with polymer molecular weight (all the samples were crystallized at 100°C).

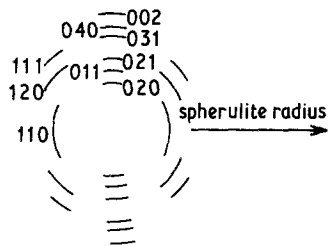
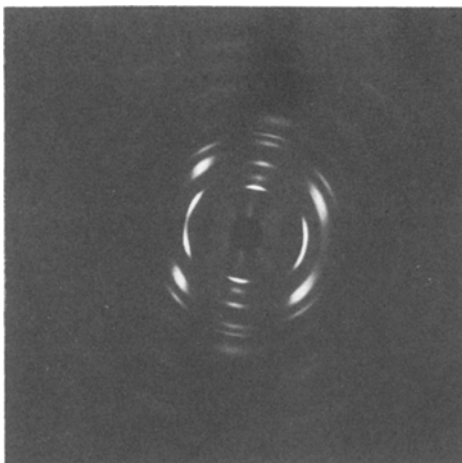


Figure 5 Selected area X-ray diffraction pattern together with a sketch showing the indexing of the spots from part of a PHB spherulite. The radius of the spherulite is horizontal in this pattern.

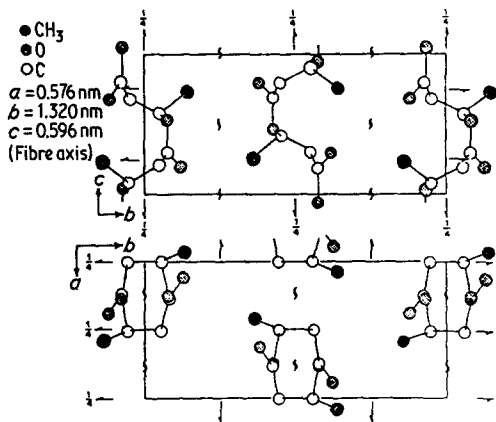
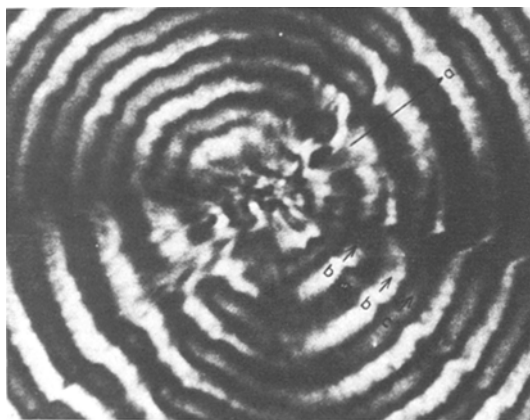


Figure 6 A diagram indicating the orientation of the crystal axes in a PHB spherulite. On the left we have superimposed the crystal axes on a photograph of a spherulite; on the right we have reproduced a diagram of the molecules in the unit cell.

cases the crystals appear to have a three-dimensional tent-like structure. Selected area diffraction from part of a crystal indicates that the crystallographic  $a$ -axis runs along the long direction of each crystal. This is illustrated in Fig. 10. We have also seen that when crystals fracture, fibres are drawn out across the short direction of the crystals, while cracks

along the crystal length are free of such fibres. In Fig. 11 we show this effect in a preparation of crystals which were deliberately fractured by depositing them on Mylar films which are stretched by 50% before the crystals were removed using polyacrylic acid [23]. The behaviour suggests the direction of chain folding is parallel to the long axes of the crystals edges, i.e. along the  $\{00\}$  planes.

We have also measured the lamellar thickness of these solution-grown crystals both directly from shadow lengths in the electron microscope and by low angle X-ray diffraction studies on sedimented mats. The shadow length measurements are subject to considerable error owing to the thinness of the crystals, but always give results close to those from the sedimented mats. We present in Fig. 12 the results of the low angle X-ray measurements in the form of a plot of lamellar thickness against crystallization temperature. Wide angle X-ray studies of the same samples indicate that there is little or no chain tilt present.

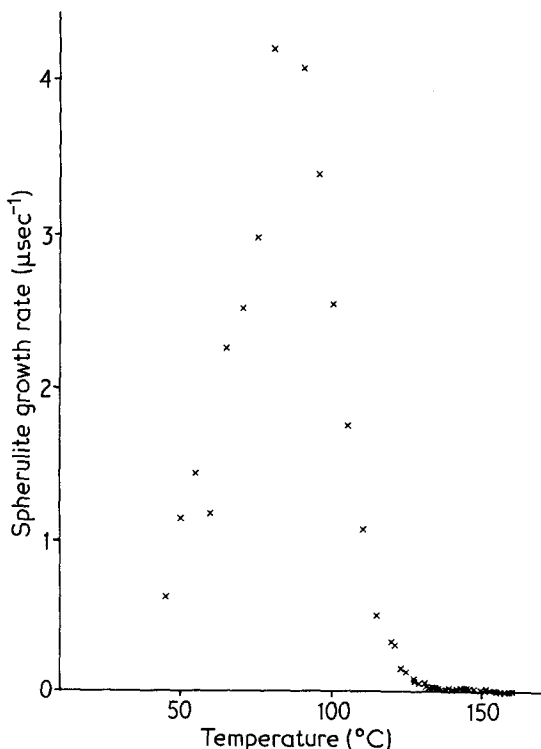


Figure 7 A graph showing the variation in spherulite growth rate with crystallization temperature.

## 2.5. Melting of PHB crystals

In all the experiments in this section we used a polymer with  $M_n = 133\,000$ ;  $M_w = 358\,000$ . Each experiment was carried out using fresh polymer so as to minimize any effects due to degradation. We recognize that PHB is susceptible to degradation in the melt: we found that in our experience after holding a melt at 190°C for *c.* 1 hour the average molecular weight had dropped to about one half of its original value. Fig. 13 shows a plot of the melting points of PHB crystals as a function

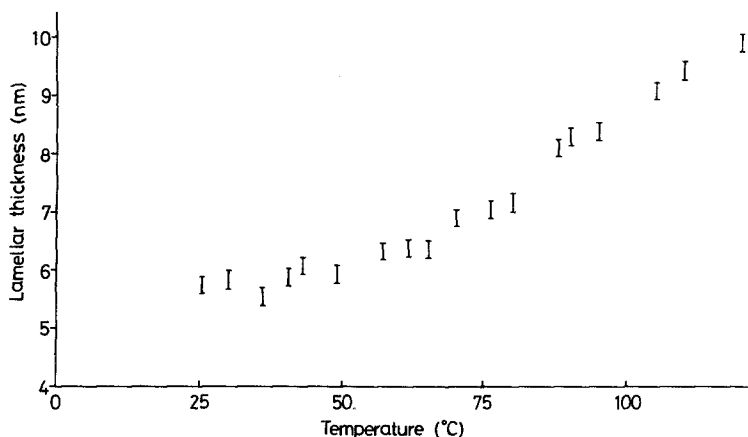


Figure 8 A graph showing the lamellar thickness of PHB as a function of the crystallization temperature.

of their crystallization temperatures. The melting points were obtained using a Mettler hot stage in the optical microscope. Note that there is a distinct peak in the  $T_c$  against  $T_m$  data at a temperature of *c.* 60°C which is always present, although not at a well-defined crystallization temperature and depending strongly on molecular weight. That this peak is a real effect can be demonstrated very simply by growing spherulites during cooling, so that the centres of the spherulites are grown at high temperatures and their outsides at low temperatures. On heating, the spherulites melt to leave the annular rings grown at *c.* 60°C surrounded by molten polymer. At crystallization temperatures above *c.* 140°C the melting point is seen to fall. We attribute this to degradation of the polymer caused by the long crystallization times used for these samples.

## 2.6. Crystallinity of PHB and the glass transition temperature

Two methods were used to estimate the glass transition temperature,  $T_g$ , one mechanical and the other dilatometric. The mechanical measurements were carried out using a torsion pendulum of our own design [24] at a frequency of *c.* 0.1 Hz. Samples for both techniques were prepared by quenching thin films from the melt at between 190 and 200°C into liquid nitrogen. The films were then stored in a freezer at *c.* -15°C for up to a week before measurements were made on them. In both methods of measurement the results are complicated by the fact that crystallization starts to occur in the PHB whenever it is heated above *c.* 10°C.

Typical results are shown in Figs. 14 and 15. Fig. 14 shows the variation in shear modulus and

loss factor,  $\tan \delta$ , measured at *c.* 0.1 Hz and at a maximum strain of *c.* 0.05% and strip-shaped specimens 10 cm × 2 mm × 0.05 mm. The accuracy of the measurement is limited by the fact that over this temperature range it is only possible to make measurements over a very few cycles on our free pendulum. Fig. 15 shows the results of the dilatometric measurements in the form of a plot of specific volume against temperature. The specific volume at -10°C was determined separately using a specific gravity bottle and all the other results were normalized to that value.

From these measurements we can make some estimate of the value of the glass transition temperature. The mechanical data suggest that at 0.1 Hz  $T_g$  lies between -5 and +5°C and the dilatometric results suggest  $T_g$  lies between -4 and +1°C.

We are able to calculate mass fraction crystallinity from the sample density and the density of amorphous and crystalline PHB. For this purpose we made all our density measurements at 20°C and took the amorphous density to be 1.177 g cm<sup>-3</sup> (obtained from extrapolations of data such as that in Fig. 15); we took the crystalline density to be 1.260 g cm<sup>-3</sup>, obtained from the X-ray diffraction studies [15-17].

Typically the mass fraction crystallinity measured in this way for PHB samples which have been left to crystallize fully (e.g., by storage for several weeks at room temperature) lies in the range 60% to 90%.

For the heat of fusion measurements samples of PHB were annealed at 160°C until no further increase in density could be observed (a sample with initial crystallinity of *c.* 70% would reach a maximum crystallinity of *c.* 86% after approxi-

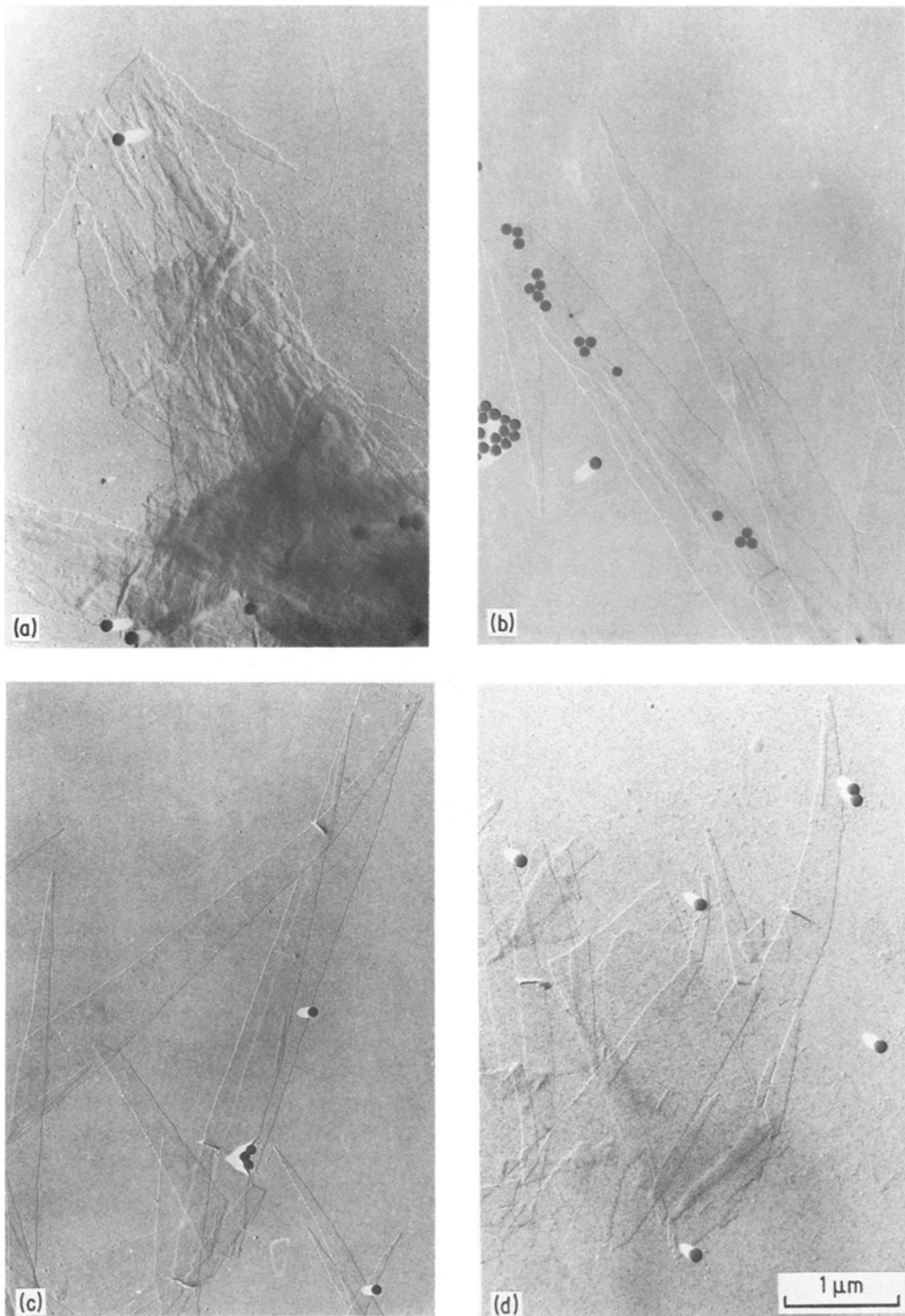


Figure 9 Electron micrographs of PHB single crystals grown from a dilute solution of propylene carbonate at various temperatures. (a)  $T_c = 36^\circ\text{C}$ ; (b)  $T_c = 50^\circ\text{C}$ ; (c)  $T_c = 69^\circ\text{C}$ ; (d)  $T_c = 83^\circ\text{C}$ . Scale as on (d).

mately one day at  $160^\circ\text{C}$ ). These annealed samples were then melted in a Perkin Elmer DSCII at very low heating rates and the heats of fusion

measured from the area under the melting endotherms. From a set of 12 such measurements we estimate the heat of fusion of PHB to be  $146\text{ J g}^{-1}$ .



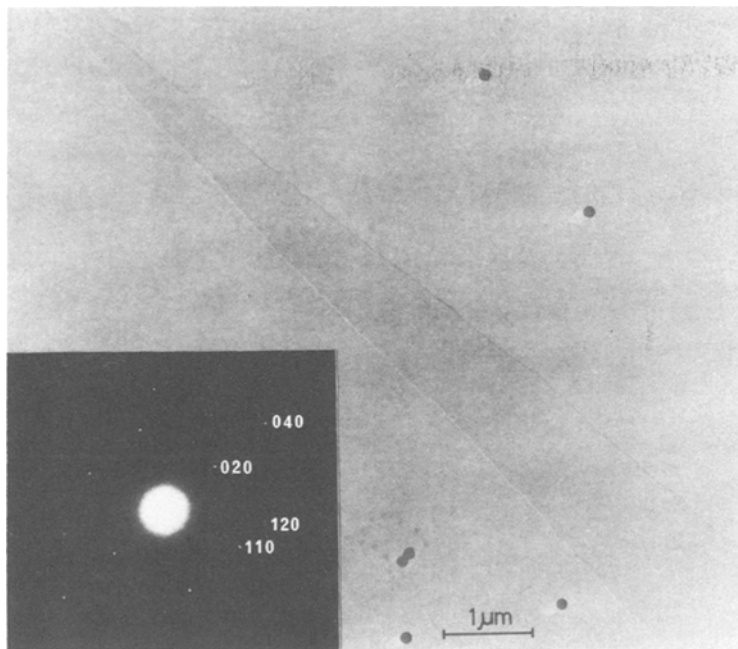


Figure 10 A PHB crystal with its electron diffraction pattern inset.

### 3. Discussion

We have tried to catalogue some of the properties of PHB and to describe the morphology of PHB crystals grown from the melt and from solution. We believe that due to the exceptional purity of PHB it would make an ideal model material for studies of nucleation and crystallization. Indeed, we have already completed a preliminary study of the nucleation behaviour of PHB [19] which has many interesting conclusions of general relevance to polymers.

The results which we have presented above have many wide-ranging implications and we shall proceed to discuss these separately. First we shall consider the data on the morphology of single crystals; secondly we shall use the data on melting of spherulitic PHB to make estimates of the equilibrium melting point and end surface free energy of PHB crystals; and finally we shall consider the implications of the spherulitic growth rate data for the latest theories of crystal growth.

#### 3.1. Morphology of solution-grown single crystals

The work on the morphology of PHB single crystals has revealed that the crystals have rough edges and that the chains apparently fold parallel to the long axis of the crystals, the crystallographic  $a$  axis. The elongated shape of these

crystals is reminiscent of lath-like polypropylene single crystals [25] where the chains are believed to fold parallel to the long edges of the laths. This direction of folding has led to difficulty in envisaging the actual growth process of such crystals, since it is usually accepted that polymer crystals grow by means of the spreading of patches of chain-folded molecules along a surface. Such a mechanism would normally lead to crystals which grow at constant shape, i.e. in a direction normal to the plane in which the chains fold.

The PHB crystals thus present an intermediate stage between the extremes of the "lath-like" polypropylene crystals and the conventional, approximately equiaxed crystals, as grown in polyethylene. Further study of the development of such PHB crystals and of the direction and regularity of chain folding within them thus promises to throw significant new light on an old problem.

A notable feature of the crystals is the unusually low values for the lamellar thickness. At the lowest crystallization temperatures from the melt the lamellar thickness is in the range of 5 to 6 nm, while from solution it is close to 4 nm. The latter only allows for 6 or 7 repeat units per fold stem, which in combination with the observed values of crystallinity leaves little scope for looseness in the fold structure, a much debated and topical issue.

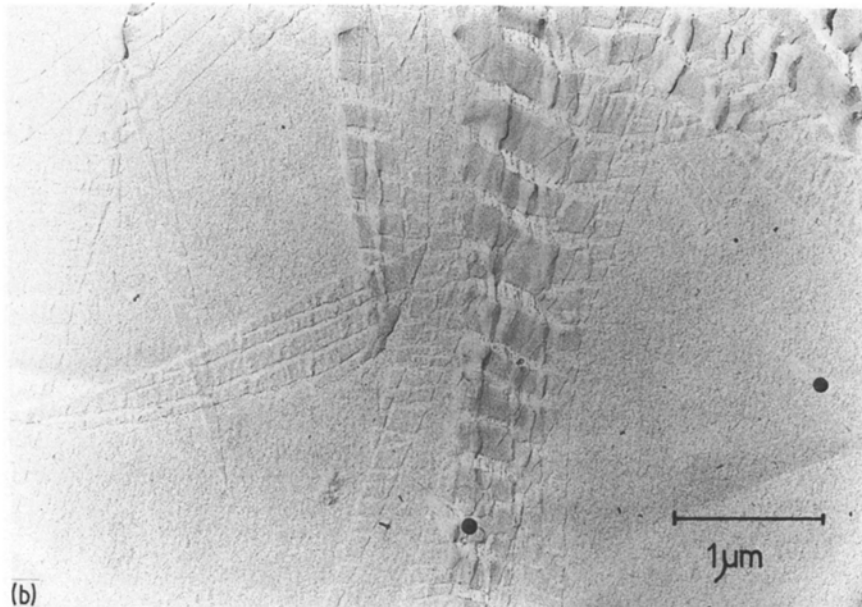
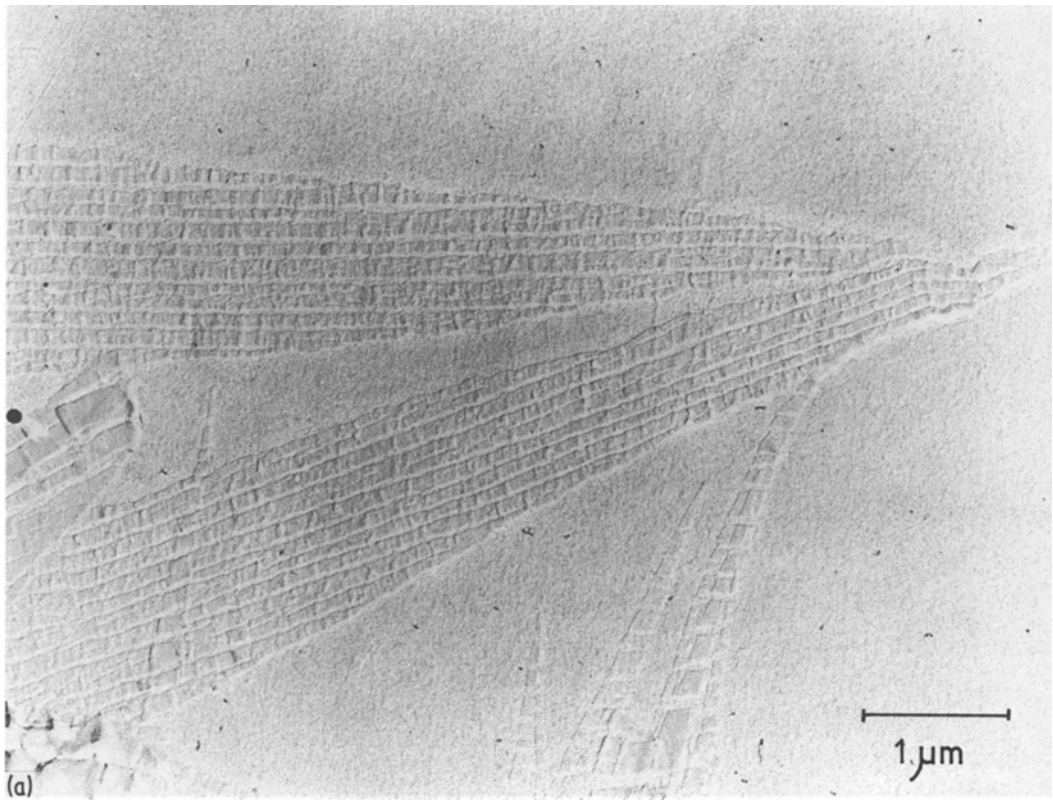


*Figure 11* Electron micrograph of deliberately fractured PHB crystals. Note that fibres are only drawn across cracks normal to the short dimension of the crystals . Crystals, fracture cleanly along their long axes.

### 3.2. Estimation of the equilibrium melting point of PHB crystals

We may estimate the equilibrium melting point,

$T_m^0$ , of an infinite PHB crystal by a variety of techniques. First we may plot the crystal melting point as a function of crystallization temperature

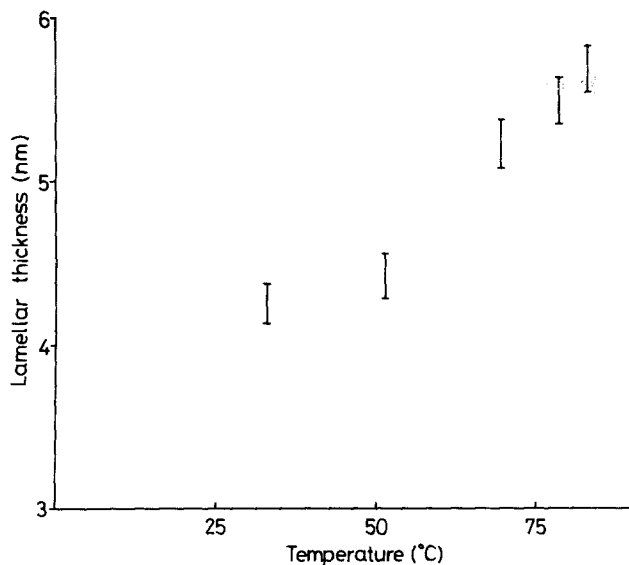


Figure 12 Graph showing the thickness of PHB single crystals grown from propylene carbonate solution as a function of the crystallization temperature.

and extrapolate the resulting line until the melting point equals the crystallization temperature. If we do this using the data in Fig. 13, but ignoring the anomalously high melting points for samples crystallized at *c.* 60°C and the low melting points observed at the highest crystallization temperatures, then we find the equilibrium melting point,  $T_m^0$ , to be  $195 \pm 5^\circ\text{C}$ . Secondly, we may plot the crystal melting point as a function of the inverse lamellar thickness; this is based on the assumption that the depression in melting point is solely due to the finite crystal thickness in which case the crystal melting point is given by:

$$T_m = T_m^0 \left( 1 - \frac{2\sigma_e}{\Delta H l} \right) \quad (2)$$

where  $T_m$  is the observed melting point,  $\sigma_e$  the fold surface free energy,  $\Delta H$  the heat of fusion and  $l$  the lamellar thickness. We have combined the data in Figs. 8 and 13, again ignoring the anomalous data in Fig. 13, and replotted them in Fig. 16 as the melting point as a function of inverse lamellar thickness. From the intercept of this line we find  $T_m^0 = 200 \pm 5^\circ\text{C}$  and from the slope that  $\sigma_e/\Delta H = 2.06 \times 10^{-10} \text{ m}^{-1}$ , taking  $T_m^0 = 470 \text{ K}$ ; thus if we use our estimate of  $\Delta H = 1.85 \times 10^8 \text{ J m}^{-3}$  we find  $\sigma_e = 38 \pm 6 \times 10^{-3} \text{ J m}^{-2}$ . A third estimate for  $T_m^0$  may be obtained from the fitting of the growth rate data to a theoretical relationship as described in the next section. This leads to a best fit value of  $197 \pm 2^\circ\text{C}$ , which, since it lies between the other two estimates, is the value we prefer.

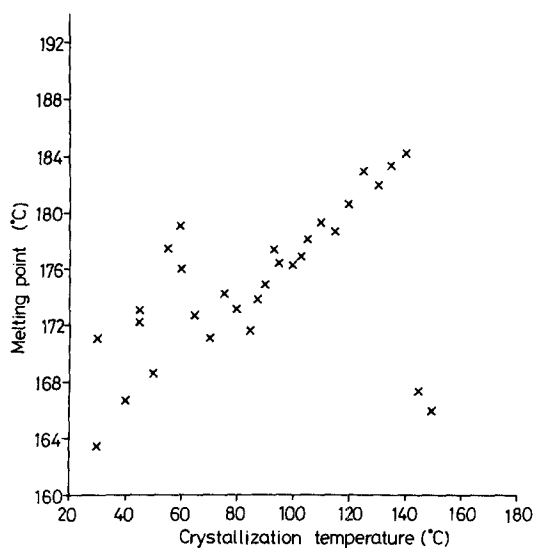


Figure 13 A graph showing the variation in spherulite melting point as a function of crystallization temperature.

### 3.3. The growth rate of PHB spherulites

Hoffman [26] gives the linear growth rate of spherulites as:

$$G = G_0 \exp \left[ - \frac{U^*}{R(T - T_\infty)} \right] \times \exp \left( - \frac{K\sigma_e T_m^0}{\Delta H \Delta T k T} \right) \quad (3)$$

where  $G_0$  is the constant,  $U^*$  is an activation energy for transport of molecules to the growth front,  $R$  is the gas constant,  $T$  is the crystallization temperature,  $T_\infty$  is the temperature below which molecules become immobile,  $\Delta T$  is the super-

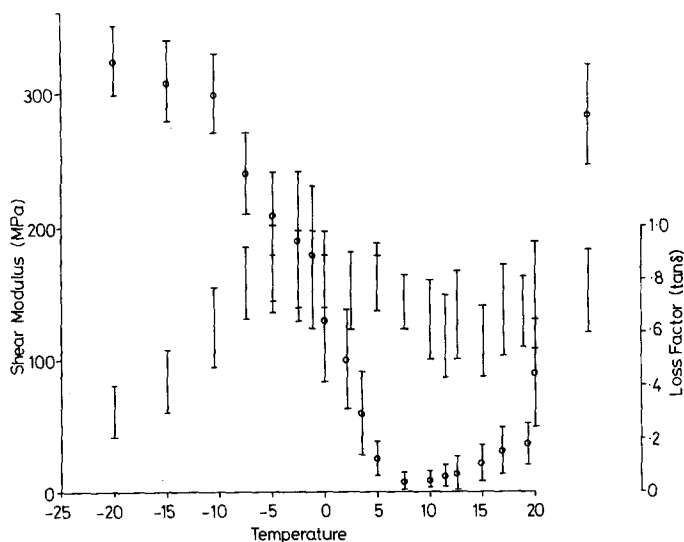


Figure 14 A graph showing the variation of the shear modulus and loss factor as an amorphous specimen of PHB is heated up from  $-25^{\circ}\text{C}$ . The ringed symbols refer to the modulus measurements.

cooling,  $k$  is Boltzmann's constant,  $\sigma$  is the side surface free energy, and  $K$  may have the value 2 or 4 depending on the growth mechanism. Hoffman proposes that there are three distinct regimes of growth of polymer crystals, depending on the relative rates of formation of new secondary nuclei on the growth front and the rate at which the nuclei once formed spread along the growth front. At low supercoolings the rate of spreading is so large compared with the rate of nucleation that a nucleus once formed spreads right across the growth front: Regime I. At higher supercoolings several nuclei form and spread across the growth front together, the separation between them decreasing as the supercooling increases: Regime II. At a sufficiently high supercooling the separation

is of the order of the molecular width, when no more spreading takes place: Regime III. The three regimes may be distinguished by the value of the constant  $K$  in Equation 3; in Regimes I and III it takes the value 4 and in Regime II it takes the value 2. This latest theory due to Hoffman differs from all earlier theories in that it introduces the third regime (Regime III) at high supercoolings.

We may use our data on spherulite growth rates shown in Fig. 7 to attempt to fit such a relationship. To do this we need to know  $T_m^0$ ,  $U^*$  and  $T_\infty$ . At high crystallization temperatures the term  $\exp[-U^*/R(T-T_\infty)]$  is small and essentially constant. We may therefore use our data to find a value for  $T_m^0$  (obviously we look for a value close to the estimates described above). The best

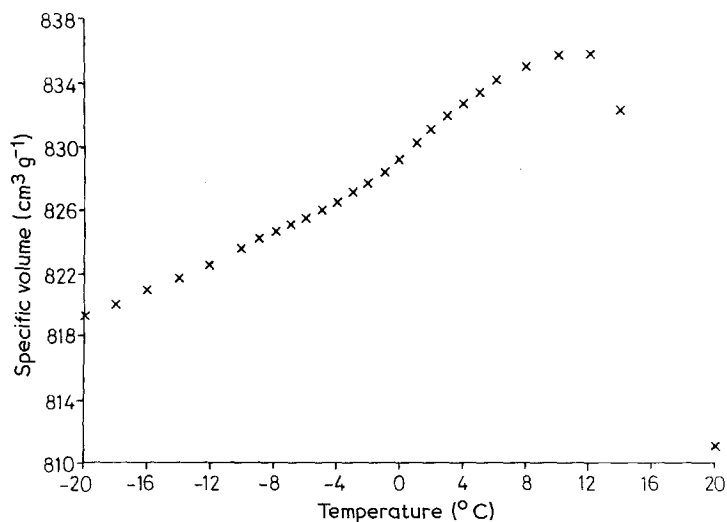


Figure 15 A graph showing the changes in specific volume during heating of a glassy PHB specimen.

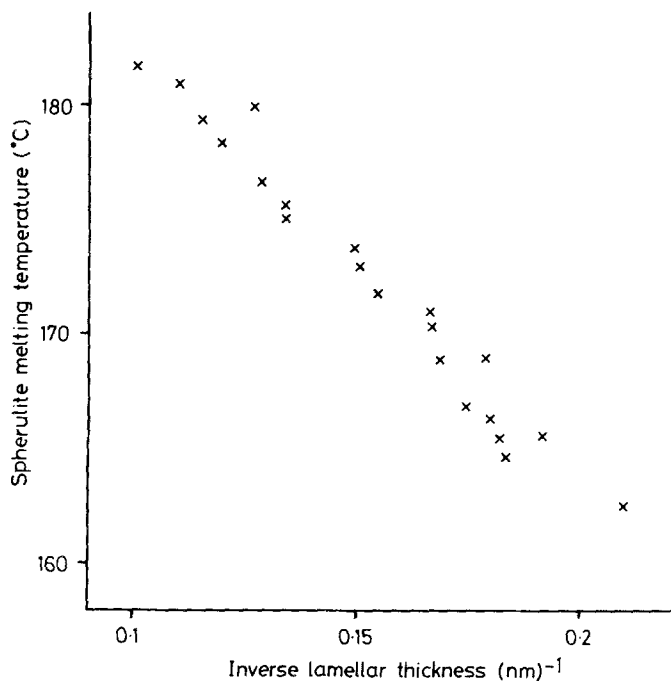


Figure 16 A graph, compiled from the data in Figs. 8 and 13, showing the variation in spherulite melting temperatures as a function of the inverse lamellar thickness.

linear plot of  $\log G$  against  $1/T\Delta T$  is obtained with  $T_m^0 = 197^\circ\text{C}$ . If we now turn to the data on low crystallization temperatures we may attempt to estimate  $U^*$  and  $T_\infty$ . We expect  $T_\infty$  to be approximately  $50^\circ\text{C}$  below the glass transition temperature so by taking  $T_\infty$  initially as  $-50^\circ\text{C}$  and then optimizing both  $U^*$  and  $T_\infty$  to obtain good linear plots for the low crystallization temperature data we find the best fits with  $U^* = 10.25\text{ kJ mol}^{-1}$  and  $T_\infty = -48^\circ\text{C}$ . We have plotted our growth rate data in the form  $\log G + U^*/R(T - T_\infty)$  against  $1/T\Delta T$  in Fig. 17. The most

notable feature of this figure is the change of slope at a crystallization temperature of *c.*  $130^\circ\text{C}$ . The slope of line for the low crystallization temperatures (up to  $128^\circ\text{C}$ ) is  $-4.99 \pm 0.02 \times 10^5\text{ K}^2$ , while that for the high crystallization temperatures (above  $135^\circ\text{C}$ ) is  $-2.47 \pm 0.05 \times 10^5\text{ K}^2$ .

We interpret this as a change in the constant  $K$  in Equation 3 from 2 at high crystallization temperatures to 4 at lower crystallization temperatures. In the terminology used by Hoffman [26] this would correspond to a Regime II–Regime III transition. Thus our data lend strong support to

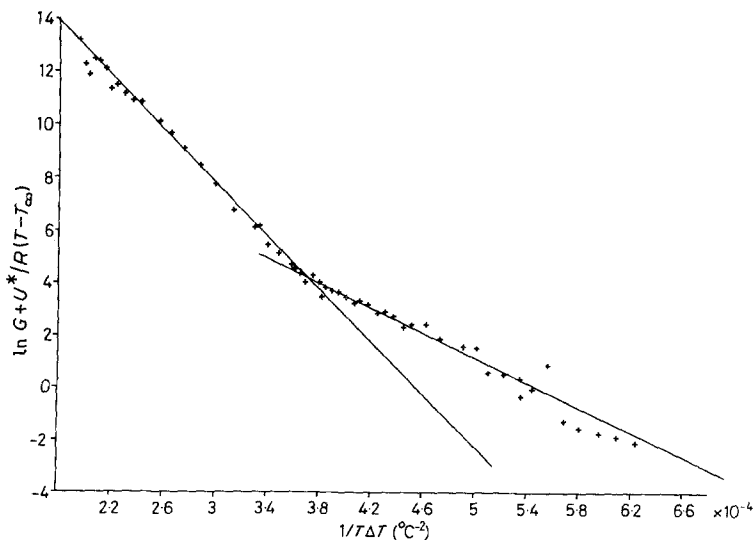


Figure 17 A plot of  $\log_e$  (growth rate)  $+ U^*/R(T - T_\infty)$  against  $1/T\Delta T$  for PHB spherulites (see text for values of  $U^*$  and  $T_\infty$ ).

the existence of Regime III as predicted by Hoffman.

#### 4. Conclusion

The purpose of this paper was to draw attention to the availability of a new and potentially extremely useful model polymer system for crystallization studies. PHB being very pure contains only few nuclei for crystallization. This allows both the exploration of a large range of supercoolings and the attainment of very large spherulites, features which are useful for studies of crystallization and morphology. Amongst the morphological features are the unusual crystal habits and extreme thinness of lamellae, both relevant to current issues on chain folding. The wide range of supercoolings at which crystallization can be conducted has enabled possibly the clearest demonstration of a Regime II to III transition in support of latest theoretical postulates [26].

#### Acknowledgements

The authors would like to thank Dr W. S. Fulton for the diffraction pattern shown in Fig. 5.

#### References

1. M. LEMOIGNE, *Ann. Inst. Past.* **39**, (1925) 144.
2. J. MERRICK, *Photosynth. Bact.* **199** (1978) 219.
3. E. A. DAWES and P. J. SENIOR, *Adv. Microbiol.* **10** (1973) 138.
4. J. S. HERRON, J. D. KING and D. C. WHITE, *Appl. Environ. Microbiol.* **35** (1978) 251.
5. N. G. CARR, *Biochem. Biophys. Acta* **120** (1966) 308.
6. L. L. WALLEN and W. K. ROHWEDDER, *Environ. Sci. Technol.* **8** (1974) 576.
7. A. C. WARD, B. I. ROWLEY and E. A. DAWES, *J. Gen. Microbiol.* **102** (1977) 61.
8. D. G. LUNDGREN, R. ALPER, C. SCHNAITMAN and R. H. MARCHESSAULT, *J. Bacteriol.* **89** (1965) 245.
9. P. A. HOLMES, L. F. WRIGHT and B. ALDERSON, European Patent Application 15123 (1979).
10. J. N. BAPTIST, US Patent 3044 942 (1962).
11. *Idem*, US Patent 3036 959 (1962).
12. R. M. LAFFERTY, *Chem Rundsch.* **30** (1977) 15.
13. D. ELLAR, D. G. LUNDGREN, K. OKAMUARA and R. H. MARCHESSALT, *J. Mol. Biol.* **35** (1968) 489.
14. R. H. MARCHESSAULT, S. COLOUMBE, H. MORIKAWA, K. OKAMURA and J. F. REVOL, *Canad. J. Chem.* **59** (1981) 38.
15. J. CORNIBERT and R. H. MARCHESSAULT, *J. Mol. Biol.* **71** (1972) 735.
16. M. YOKOUCHI, Y. CHATANI, H. TADAKORO, K. TERANISHI and H. TANI, *Polymer* **14** (1973) 267.
17. K. OKAMURA and R. H. MARCHESSAULT, in "Conformational aspects of Biopolymers", Vol. II, edited by G. N. Ramachandran (Academic Press, London and New York, 1967).
18. E. R. HOWELLS, *Chem. Ind.* (1982) 508.
19. P. J. BARHAM, *J. Mater. Sci.* **19** (1984) in press.
20. L. HUGHES and K. R. RICHARDSON, European Patent Application 46 344 (1982).
21. J. BRANDRUP and E. H. IMMERGUT, "Polymer Handbook" (Wiley Interscience, New York, 1966).
22. S. ATIKA, Y. EINDGA, Y. MIYAKI and H. FUKITA, *Macromolecules* **9** (1976) 774.
23. P. H. GEIL, "Polymer Single Crystals" (Interscience, New York, 1963).
24. R. G. C. ARRIDGE and P. J. BARHAM, *Polymer* **19** (1978) 603.
25. J. A. SAUER, D. R. MORROW and G. C. RICHARDSON, *J. Appl. Phys.* **36** (1965) 3017.
26. J. D. HOFFMAN, *Polymer* **24** (1983) 3.

Received 12 September  
and accepted 29 September 1983